Results in Physics 28 (2021) 104592

Contents lists available at ScienceDirect

Results in Physics

journal homepage: www.elsevier.com/locate/rinp

Dynamic modulation of slow light rainbow trapping and releasing in a tapered waveguide based on low-symmetric photonic crystals

Changsheng He [a], Hong Wu [a,*], Yanhui Feng [b], Wei Su [c], Feng Li [a]

[a] School of Science, Nanjing University of Posts and Telecommunications, Nanjing, Jiangsu 210023, China
[b] School of Management, Nanjing University of Posts and Telecommunications School, Nanjing, Jiangsu 210023, China
[c] College of Science, Hohai University, Nanjing, Jiangsu 210098, China

ARTICLE INFO

Keywords:
Slow light
Rainbow trapping
Photonic crystal waveguide

ABSTRACT

We propose a numerical investigation of slow light rainbow trapping and releasing in a tapered photonic crystal waveguide which is formed by linearly modifying the structural parameters in low-symmetric photonic crystals. Through dispersion analysis and numerical simulations, the electromagnetic waves of different frequencies in a normalized bandwith of ~5% can be trapped at different positions, as called "rainbow trapping". Moreover, the tapered photonic crystal waveguide is created on polystyrene subtract, of which refractive index can be adjusted by tuning the external voltage based on electro-optic effect. Therefore, when the applied voltage is properly modulated, the trapped wave will be captured in different positions even released. The structure has broad application prospects in optical switch, wavelength-division multiplexing, and other optical communication devices.

Introduction

Recently, slow light has been investigated by many researchers, thanks to its promising properties in optical storage, optical caching, optical information processing and other areas [1–5], which are considered to be the key technologies for future all-optical communication and information storage. Initially, slow light was realized based on quantum effects such as electromagnetically induced transparency (EIT), coherent population oscillation (CPO), stimulated Raman scattering (SRS) and stimulated Brillouin scattering (SBS) [6–9]. However, the ultra-low working temperature/pressure and the narrow working bandwidth limited their practical implementations. As a new artificial material to realize slow light, photonic crystals (PCs) have attracted much attention because of their support for room-temperature and their fine device miniaturization [10–14]. In order to obtain wide working bandwidth for practical applications, many efforts have been made in obtaining flat bands on dispersion curves by locally modifying the effective index of PCs [15]. Recent reports on slow light "rainbow trapping" in some artificial materials (such as PCs, metamaterials, etc.) have opened a new way to slow down the speed of light over a wide frequency range [16–18].

Rainbow trapping refers to the trapping of electromagnetic waves of different wavelengths in different spatial locations, just like sunlight scattering into a continuous color spectrum through a prism (hence the name rainbow). Since the first theoretical work was reported, many researchers have been trying to find different ways to realize rainbow trapping. For instance, metallic grating structures, topological PCs and chirped PCs [19–28]. When analyzing the previous researches, we found that most of the implementations are based on metallic materials or graphene-dielectric compositions [29,30]. It is well known that metallic structures are lossy at optical wavelengths, and gain is usually introduced to compensate for the loss. In addition, the complex fabrication process of graphene makes the fabrication of graphene-based optical devices more complicated. Considering these two issues, we think that using all-dielectric structure may be a superior alternative for rainbow trapping.

In modern information technology, it is necessary to adjust the trapping properties after the device is fabricated. For example, optical switches need to trap and release the electromagnetic waves under external commands, which can be controlled as an "off" and "on" mode by actively adjusting some conditions. Unfortunately, most rainbow trapping structures cannot be tuned once they are fabricated. In Ref. [31], a chirped PCs using all-dielectric materials was proposed, the distance between each neighboring column of dielectric rods has been

* Corresponding author.
E-mail address: wuhong@njupt.edu.cn (H. Wu).

https://doi.org/10.1016/j.rinp.2021.104592
Received 16 May 2021; Received in revised form 15 July 2021; Accepted 19 July 2021
Available online 22 July 2021

linearly increased along the propagation direction, finally, a broadband rainbow trapping was achieved. In Ref. [32], a tapered PC waveguide composed of alumina cylindrical rods was reported to slow down and trap the propagating light. However, the common disadvantage of these two structures is that they cannot modulate the rainbow trapping and releasing without changing the structures.

In general, some physical effects can realize the dynamic modulation of PC devices, including electro-optic effects [33], magneto-optic effects [34] and thermo-optic effects [22]. Among all these methods, electro-optical materials have been widely used since they have a high electro-optical coefficient and nanosecond electro-optical response. In this paper, a tapered PC waveguide composed of dielectric rods is created on a polymer substrate; the polymer is highly nonlinear electro-optic polystyrene ($n_{poly} = 1.6$). We demonstrate theoretically and numerically that electromagnetic waves of different frequencies in the wideband region can be trapped at different positions. Meanwhile, the optical properties of polystyrene can be adjusted by tuning the external voltage [33,35]. Therefore, when the applied voltage is changed, the trapped wave will continue to propagate and be captured in other positions, or even be released and outputted from the edge of the waveguide. The structure has broad application prospects in optical switch, wavelength-division multiplexing, and other optical communication devices.

Structure design and dispersion analysis

As shown in Fig. 1, the two-dimensional (2D) low-symmetric PC is created on a polymer substrate ($n_{poly} = 1.6$). Two basic dielectric rods ($n_{si} = 3.75$) with the radii of $R = 0.2a$ and $r = 0.1a$ fill the square-lattice holes on the polymer substrate, where a is the lattice constant. The bigger rods are located at the unit-cell center and the smaller ones are placed $0.35a$ away from the center along the y-direction. According to the dispersion analysis using 2D plane-wave expansion (PWE) method, the photonic band gap (PBG) of this PC structure lies between normalized frequencies 0.2453 ($2\pi c/a$) and 0.2927 ($2\pi c/a$) for transverse magnetic (TM) polarization. To form the PC waveguide, a mirrored copy of the PC is created along the y-direction. Therefore, a mirror-symmetrical waveguide is constructed and the waveguide width W can be adjusted by moving two PC regions.

Firstly, it is necessary to study the influence of structural parameters on waveguide modes. Based on previous work, such parameters including the waveguide width W, positions and sizes of the first two rows of the elements, and so on [31]. Considering the difficulty of theoretical design and experimental preparation, we will modify the positions of the first row of smaller elements, while W is fixed at $1.54a$.

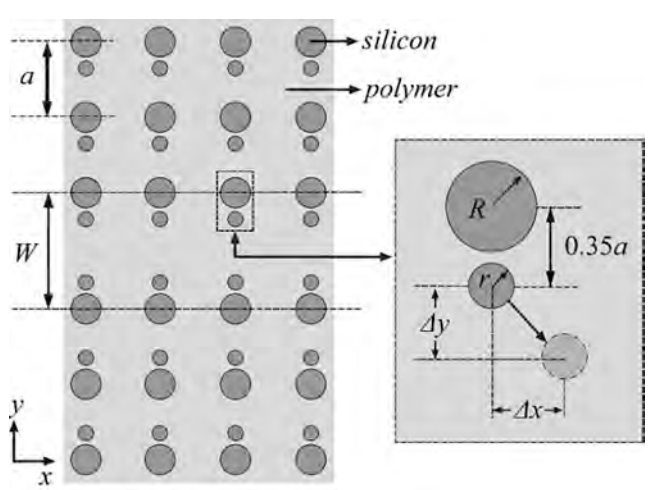

Fig. 1. Schematic representation of the proposed PC structure based on polymer and its structural parameters.

As can be seen from Fig. 1, Δx represents the horizontal moving distance, Δy represents the vertical moving distance, and when the smaller elements move from the bigger ones, Δy is positive, otherwise, it is negative. In Fig. 2(a) and (b), the band diagram analyses of the structure at specific locations are presented. When Δx is kept at zero and Δy is increased (corresponding to Fig. 2(a)), the band curves move down and keeping the slope almost constant. However, the situation changes when Δy is kept at zero and Δx is increased (corresponding to Fig. 2(b)). In this case, the rear of each curve near the edge of Brillouin zone is more affected than the front. As a result, the slopes of the bands vary between positive and negative, and the inflection points emerge when Δx is near $0.2a$ or beyond.

As is well known, the group velocity (defined as $v_g = \partial\omega/\partial k$) of a guided mode can be obtained from the slope of the dispersion curve, and the calculated results have been shown in Fig. 2(c) and (d). To minimize out-of-plane losses of slab, we only focus on the waveguide modes under the light-line. Evidently, the group velocities maintain around 0.2c for different Δy in Fig. 2(c). When we select two frequencies (0.29 ($2\pi c/a$) and 0.28($2\pi c/a$)) in the dispersion curves corresponding to $\Delta y = -0.10a$ and $\Delta y = 0.15a$ in Fig. 2(a) for modal-field distribution simulation, it is found that the distribution of fast-light mode does not change with Δy. Then we turn to the case in Fig. 2(d). When Δx is $0.2a$ or beyond, extremely small or even zero group velocity occurs near the inflection points of the dispersion curves. According to the field patterns as shown in Fig. 2(b), the slow-light mode (corresponding to the inflection frequency of 0.282 ($2\pi c/a$) for $\Delta x = 0.5a$) shows more obvious mode compression for the lateral field distribution than the fast-light mode. Unfortunately, the uniform waveguide (with fixed Δx and Δy) can only slow down the group velocity within a rather narrow bandwidth near the inflection point, which hinders further improvement of slow-light capacity.

Based on the above analysis, on the one hand, we found that the most efficient reduction of the group velocity occurs when the frequency approaches to the inflection point of a given Δx. It means that the electromagnetic wave incident at a specific frequency will propagate in the waveguide at a very small group velocity, or even be trapped. On the other hand, the increase of Δy can make the dispersion curve move down rapidly while maintaining the shape. Therefore, to broaden the spectral region where light signal can be trapped, a tapered PC waveguide by linearly increasing Δy while keeping Δx as a constant is proposed, as illustrated in Fig. 3(a). Here, Δx is set as $0.5a$, Δy is chosen to gradually increase from $-0.14a$ to $0.15a$ by a fixed step of $0.01a$. When a = 440 nm, the proposed waveguide is 12.94 μm long and 4.38 μm wide. Fig. 3(b) showns linear change of Δy along the x-direction.

Fig. 4(a) shows the dispersion curves for three cases of $\Delta y = -0.08a$, 0, $0.11a$, corresponding to three different positions of $x = 2.67$ μm, 6.24 μm, and 11.15 μm, respectively. Fig. 4(b) shows the group velocities for these three cases. It can be seen that extremely small or even zero group velocities occur near three specific points marked with I, II and III, which represent the normalized frequencies of 0.287 ($2\pi c/a$), 0.284 ($2\pi c/a$) and 0.278 ($2\pi c/a$), respectively. It means that the electromagnetic wave fixed at these specific frequencies can be trapped at specific transmission locations, which are corresponding to the waveguide position x. Fig. 4(c) summarizes the theoretical prediction results of the trapped positions of electromagnetic waves at various frequencies within the range of 0.276 ($2\pi c/a$) to 0.29 ($2\pi c/a$). On the one hand, it means that the electromagnetic waves of different frequencies in a normalized bandwidth of ~5% can be "rainbow trapped" in this tapered waveguide. On the other hand, compared with the uniform waveguide with fixed Δx and Δy, the bandwith supporting the extremely slow light has been greatly broadened in this tapered waveguide, which can promote the design of large capacity optical buffer devices.

In order to verify above results, numerical simulations are performed using the two-dimensional finite-dimensional time-domain (FDTD) method with a boundary conditions of perfectly matching layers. Fig. 4 (d) illustrates the electric field distributions in x–y plane for incident

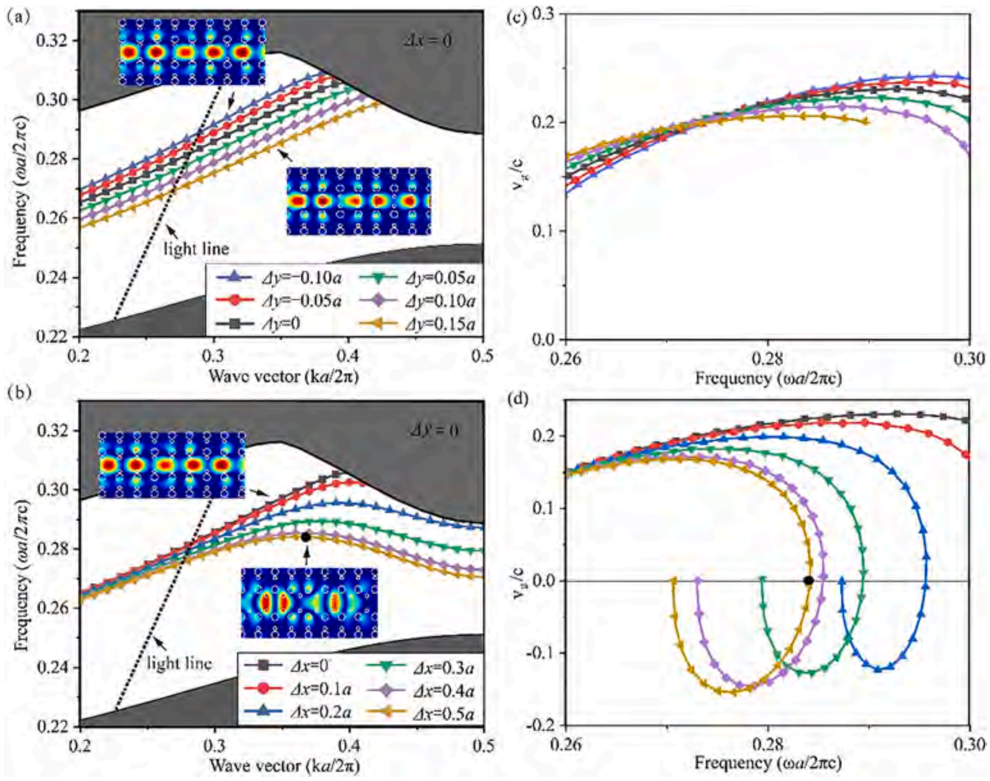

Fig. 2. Dispersion relations and group velocity of PC waveguide. (a) The dispersion curves and the corresponding (c) group velocities for different Δy. (b) The dispersion curves and the corresponding (d) group velocities for different Δx.

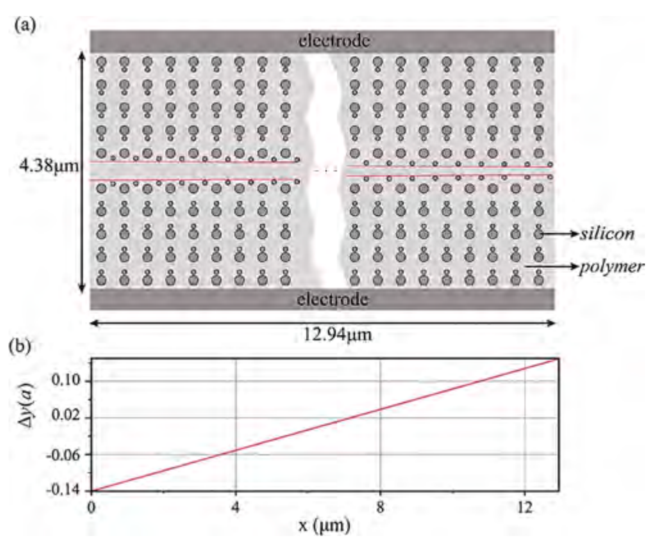

Fig. 3. (a) Schematic representation of the tapered PC waveguide. (b) Graph of linear change in the vertical moving distance Δy along the x-direction.

wavelengths of 1.53 μm, 1.55 μm, and 1.58 μm, which corresponds to the specific frequencies with zero group velocities marked with I, II, and III in Fig. 4(b), respectively. It can be found that the incident waves are trapped at different positions along the waveguide which result in "rainbow trapping". Obviously, the electric field intensity attains its maximum value closing to the corresponding trapping position. Therefore, this kind of tapered PC waveguide can be used for temporary storage of light.

Switchable slow light rainbow trapping

Once the wave is trapped, the problem we face is how to release the trapped wave at different positions in our proposed waveguide. To do that, the polymer subtract is polystyrene, whose refractive index can be adjusted by Pockels effect in the presence of an external voltage. Thus, two electrodes are placed on each side of the waveguide as shown in Fig. 3. The refractive index of variation can be calculated as [33,35] $\Delta n = -\frac{1}{2} \times n_{poly}^3 \times \gamma_{33} \times \frac{U}{d}$. Where γ_{33} is the electro-optic coefficient, U is the applied voltage, and d is the distance between the two electrodes.

In slow light PC waveguide, the nonlinear effects can be greatly enhanced due to the compression of local density of states. In this case, the electro-optic coefficient becomes $\gamma_{33} \times f^3$, where f is the local-field factor, which can be calculated as $f = \sqrt{v_g^{BULK}/v_g^{PC}}$. Where v_g^{BULK} and v_g^{PC} are group velocity in the bulk polystyrene and in the PC waveguide, respectively. Thus, the refractive index variation can be expressed as $\Delta n = -\frac{1}{2} \times n_{poly}^3 \times \gamma_{33} \times f^3 \times \frac{U}{d}$. Here, we set $n_{poly} = 1.6$, $f = 2.89$, $\gamma_{33} =$ 80 pm/V and d = 4.38 μm.

Fig. 5(a) shows the shift of the guided mode due to different applied voltages for $\Delta x = 0.5a$ and $\Delta y = -0.8a$. It is clear that, the mode moves to higher frequency with the increase of external voltage. Meanwhile, the inflection point undergoes blueshift. It means that, with the increase of propagation distance, the electromagnetic wave fixed at a specific frequency can obtain continuous modulation between the slow light trapped state and large group velocity release state. In addition, the trapped positions can be shifted with the increasing voltage. Fig. 5(b) shows the relationships between different incident frequencies and the corresponding trapped positions at different voltages of 0, 55 V, and 177 V. It can be found that the trapping positions for 0.288 ($2\pi c/a$) shifts from 2.67 μm to 6.25 μm when the voltage increased from 0 to 55 V. when U further increased to177V, the wave will be released from the waveguide. These theoretical predictions are verified by the FDTD simulation results in Fig. 5(c). Evidently, for cases I and II, the incident

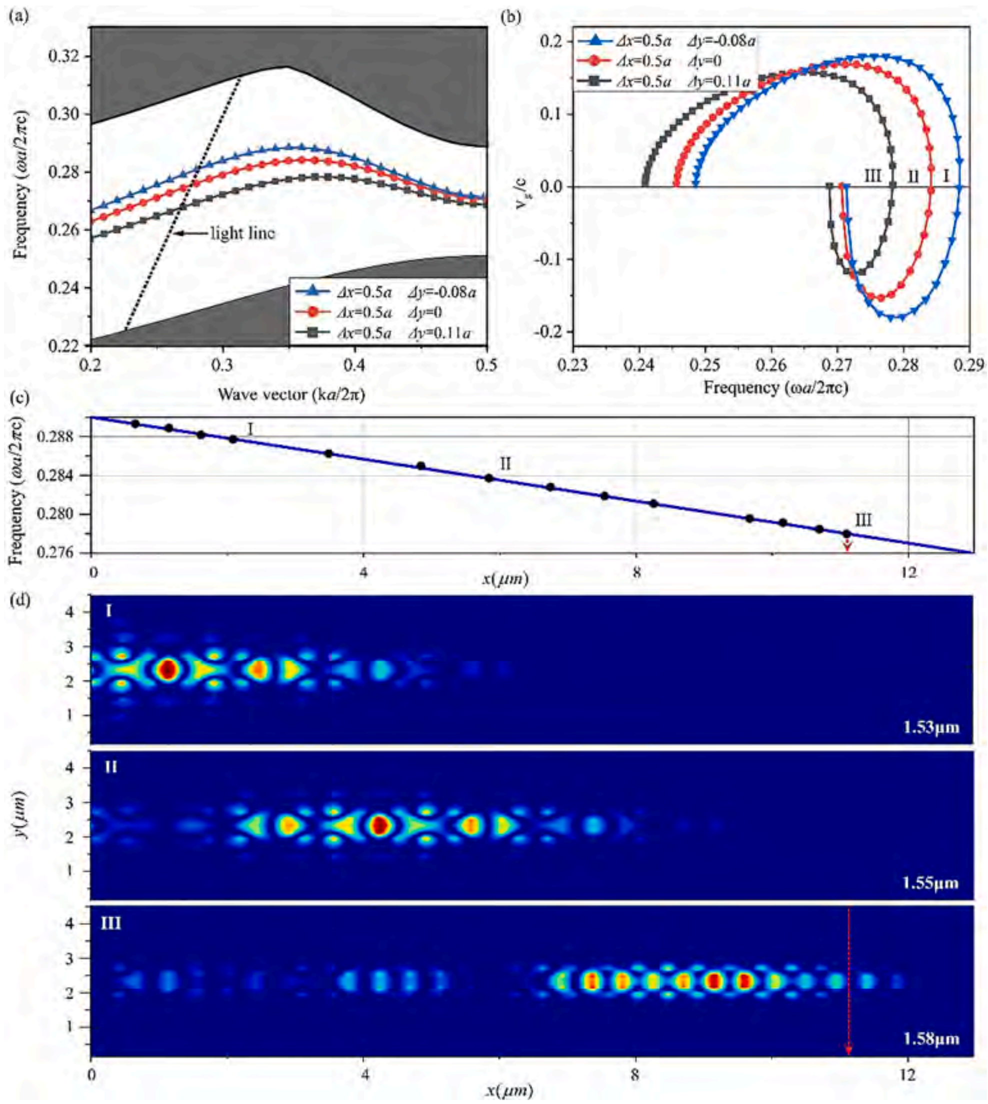

Fig. 4. (a) The dispersion curves for three cases of $\Delta y = -0.08a$, 0, 0.11a, corresponding to three different positions of $x = 2.67$, 6.24, and 11.15 μm, respectively. (b) The group velocities for different cases. (c) Trapping position as a function of cutoff frequency. (d) The electric field distributions in x–y plane for incident wavelengths of 1.53 μm, 1.55 μm, and 1.58 μm, respectively.

wave with wavelength of 1.53 μm (corresponding to normalized frequency of 0.288 ($2\pi c/a$)) maintain the maximum field intensity at specific locations, which are roughly consistent with the calculated results in Fig. 5(c). Additionally, for case III, the trapped wave is released and outputted from the edge of the waveguide. Therefore, the waveguide modes can be switched among the slow light trapped state and releasing state by tuning the external voltage.

Conclusions

Finally, it is necessary to emphasize the originality of our work. In Ref. [33], the dynamic modulation of slow light has been realized with the help of the electro-optic effect of the polystyrene substrate. In our work, the polystyrene substrate is also be used to design the photonic crystal waveguide. However, there are several differences between these two works. Firstly, owing to the different photonic crystals supporting slow light used, the mechanism of slow light effect is also different. In Ref. [33], the slow light is realized in photonic crystal coupled resonator optical waveguide (PC-CROW). The slow light in PC-CROW is based on weak coupling of located mode between cavities, so that the cavity spacing and the size of dispersion unities surrounding cavity will affect the slow light properties in PC-CROW. However, in our work, the linear-defect waveguide based on low-symmetric photonic crystal is used. The slow light of the linear-defect waveguide is due to the influence of the back scattering of the boundary on the Bloch modes induced by photonic band gap effect. Therefore, the structural parameters of the adjacent defect element have a great influence on the slow light mode. As seen from the Section 2 in our paper, the positions of the first row of smaller elements (including longitudinal movement Δx and lateral movement Δy) have been briefly studied for the dispersion analysis. It can be found that, compared with Δx, the change of Δy has a greater influence on the group velocity. The reason may be that the lateral movement Δy could produce a stronger surface mode, and the coupling between the surface mode and the Bloch mode reduces the group velocity of transmission mode, as called slow light. Secondly, in order to obtain broadband slow light effect, different solutions are used. In Ref. [33], the purpose of parameter optimization is to produce the flat-band region with nearly constant group velocity on dispersion curves. Considering both the bandwidth of flat-band region and group velocity, the slow light and buffer performance of PC-CROW can be optimized. However, in our work, the flat-band region of dispersion curve is not important. As seen from the Fig. 2(b) in Section 2, we focus on the inflection points on the

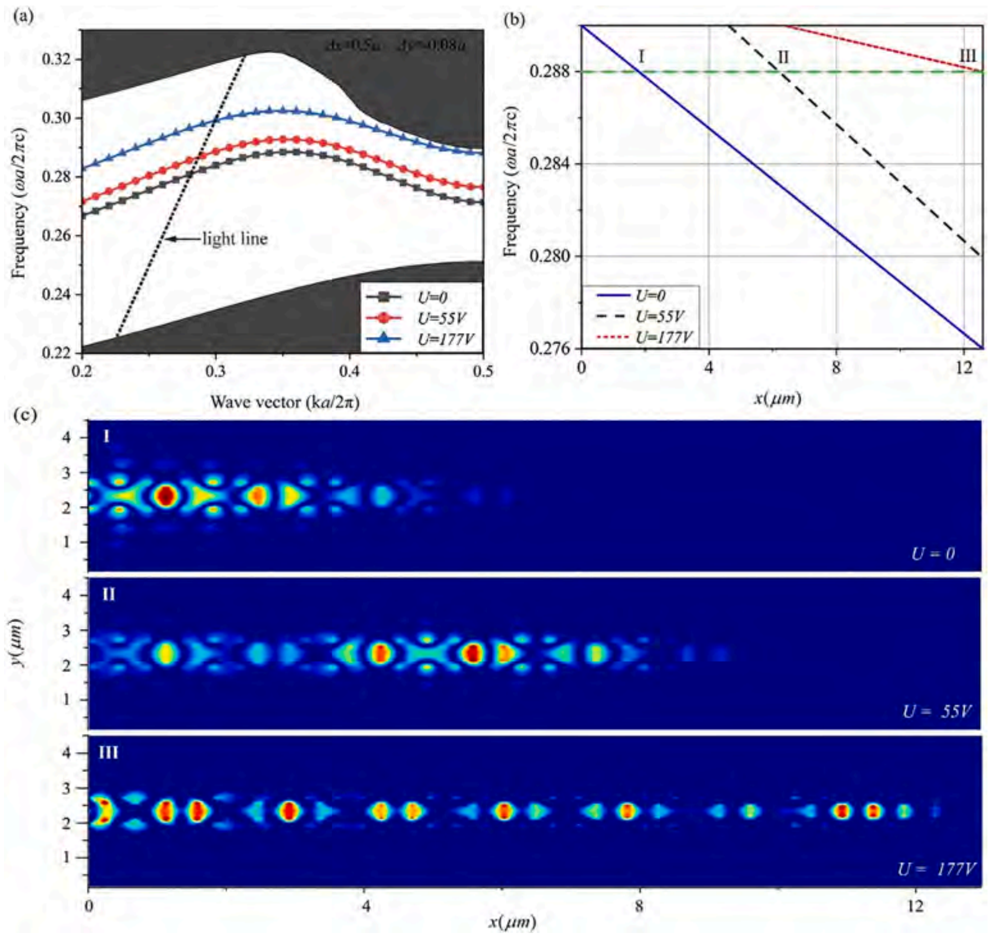

Fig. 5. (a) The dispersion curves for different applied voltages for $\Delta x = 0.5a$ and $\Delta y = -0.08a$. (b) The relationships between different incident frequencies and the corresponding trapped positions at different voltages of 0, 55 V, and 177 V. (c) The electric field distributions in x–y plane for incident wavelengths of 1.53 μm at different voltages of 0, 55 V, and 177 V.

dispersion curves when the slopes change from positive to negative. When Δx is $0.2a$ or beyond, extremely small or even zero group velocity occurs near the inflection point. We also found that, with the increasing of Δy, the inflection point can be moved to higher frequency. Therefore, to broaden the spectral region with extremely small or even zero group velocity, a tapered photonic crystal waveguide by linearly increasing Δy while keeping Δx as a constant is proposed. As a result, the electromagnetic waves of different frequencies in a normalized bandwidth of ~5% can be slowed down or even be trapped at different positions, as called rainbow trapping.

In conclusion, we present the modulation of slow light rainbow trapping and releasing using a tapered PC waveguide based on polymer substrate. To do that, the positions of the first row of smaller elements in square-lattice PC with composite elements are linearly modified to obtain a tapered waveguide. Through dispersion analysis by PWE method and numerical simulations by FDTD, the electromagnetic waves of different frequencies in the wideband region can be trapped at different positions, as called "rainbow trapping". Meanwhile, the polymer substrate is highly nonlinear electro-optic polystyrene, of which refractive index can be adjusted by tuning the external voltage based on electro-optic effect. Therefore, when the applied voltage is changed, the incident wave at a fixed frequency can be trapped in different positions, or even be released and outputted from the edge of the waveguide. The structure has broad application prospects in optical switch, optical storage, signal processing, nonlinear optical enhancement and other fields.

CRediT authorship contribution statement

Changsheng He: Conceptualization, Methodology, Data curation, Writing - original draft. **Hong Wu:** Conceptualization, Software, Validation, Writing - original draft, Funding acquisition. **Yanhui Feng:** Validation, Resources. **Wei Su:** Writing - review & editing. **Feng Li:** Writing - review & editing, Funding acquisition.

Declaration of Competing Interest

The authors declare that they have no known competing financial interests or personal relationships that could have appeared to influence the work reported in this paper.

Acknowledgements

National Natural Science Foundation of China (61605087); Natural Science Foundation of Jiangsu Province (BK20160881).

References

[1] Jafari O, Shi W, LaRochelle S. Efficiency-speed tradeoff in slow-light silicon photonic modulators. IEEE J Sel Top 2021;27(3):1–11.
[2] Kawasaki T, Mori D, Baba T. Experimental observation of slow light in photonic crystal coupled waveguides. Opt Express 2007;15(16):10274. https://doi.org/10.1364/OE.15.010274.
[3] Krauss TF. Why do we need slow light? Nat Photon 2008;2(8):448–50.
[4] Mookherjea S, Park JS, Yang S-H, Bandaru PR. Localization in silicon nanophotonic slow-light waveguides. Nat Photon 2008;2(2):90–3.

[5] Yang Sa, Zhou R-L, Huang Y-J. Surface plasmon resonance and field confinement in graphene nanoribbons in a nanocavity. Front Phys-Beijing 2021;16(4). https://doi.org/10.1007/s11467-021-1060-2.
[6] Lukin MD, Imamoğlu A. Controlling photons using electromagnetically induced transparency. Nature 2001;413(6853):273–6.
[7] John S. Strong location of photons in certain disordered dielectric superlattices. Phys Rev Lett 1987;58:2486–9.
[8] Patnaik AK, Liang JQ, Hakuta K. Slow light propagation in a thin optical fiber via electromagnetically induced transparency. Phys Rev A 2002;66(6). https://doi.org/10.1103/PhysRevA.66.063808.
[9] Vlasov YA, O'Boyle M, Hamann HF, McNab SJ. Active control of slow light on a chip with photonic crystal waveguides. Nature 2005;438(7064):65–9.
[10] Baba T. Slow light in photonic crystals. Nat Photon 2008;2:465–73.
[11] Bo F, Liu Ze, Gao F, Zhang G, Xu J. Slow and fast light in photorefractive GaAs-AlGaAs multiple quantum wells in transverse geometry. J Appl Phys 2010;108(6):063101. https://doi.org/10.1063/1.3485829.
[12] Moghaddam MK, Fleury R. Slow light engineering in resonant photonic crystal line-defect waveguides. Opt Express 2019;27(18):26229. https://doi.org/10.1364/OE.27.026229.
[13] Monat C, Ebnali-Heidari M, Grillet C, Corcoran B, Eggleton BJ, White TP, et al. Four-wave mixing in slow light engineered silicon photonic crystal waveguides. Opt Express 2010;18(22):22915. https://doi.org/10.1364/OE.18.022915.
[14] Schuller C, Klopf F, Reithmaier JP, Kamp M, Forchel A. Tunable photonic crystals fabricated in III-V semiconductor slab waveguides using infiltrated liquid crystals. Appl Phys Lett 2003;82:2767–9.
[15] Johnson SG, Joannopoulos JD. Designing synthetic optical media: photonic crystals. Acta Mater 2003;51(19):5823–35.
[16] Chaplain GJ, Pajer D, De Ponti JM, Craster RV. Delineating rainbow reflection and trapping with applications for energy harvesting. New J Phys 2020;22(6):063024. https://doi.org/10.1088/1367-2630/ab8cae.
[17] Ghaderian P, Habibzadeh-Sharif A. Rainbow trapping and releasing in graded grating graphene plasmonic waveguides. Opt Express 2021;29(3):3996. https://doi.org/10.1364/OE.414982.
[18] Neseli B, Bor E, Kurt H, Turduev M. Rainbow trapping in a tapered photonic crystal waveguide and its application in wavelength demultiplexing effect. J Opt Soc Am B 2020;37:1249–56.
[19] Arreola-Lucas A, Báez G, Cervera F, Climente A, Méndez-Sánchez RA, Sánchez-Dehesa J. Experimental evidence of rainbow trapping and bloch oscillations of torsional waves in chirped metallic beams. Sci Rep 2019;9(1). https://doi.org/10.1038/s41598-018-37842-7.
[20] Kanyang R, Zhang F, Han G, Liu Y, Shao Y, Zhang J, et al. Rainbow trapping and releasing in InSb graded subwavelength grooves by thermal tuning at the terahertz range. Opt Mater Express 2018;8:2954–66.
[21] Liu Y, Kanyang R, Han G, Shao Y, Fang C, Huang Y, et al. Rainbow trapping in highly doped silicon graded grating strip at the terahertz range. IEEE Photon J 2018;10(3):1–9.
[22] Liu Y, Wang Y, Han G, Shao Y, Fang C, Zhang S, et al. Engineering rainbow trapping and releasing in ultrathin THz plasmonic graded metallic grating strip with thermo-optic material. Opt Express 2017;25(2):1278. https://doi.org/10.1364/OE.25.001278.
[23] Shen Q, Shen L, Min W, Xu J, Wu C, Deng X, et al. Trapping a magnetic rainbow by using a one-way magnetostatic-like mode. Opt Mater Express 2019;9:4399–408.
[24] Tian Z, Yu L. Rainbow trapping of ultrasonic guided waves in chirped phononic crystal plates. Sci Rep 2017;7(1). https://doi.org/10.1038/srep40004.
[25] Wang S-L, Ding L, Xu W. Dynamic control of the terahertz rainbow trapping effect based on a silicon-filled graded grating. Chin Phys B 2017;26(1):017301. https://doi.org/10.1088/1674-1056/26/1/017301.
[26] Wang Z, Gao Z, Zhang Y, Lou J, Cheng P, Zhao H. Slowing designer surface plasmons in a surface-wave photonic crystal. Appl Opt 2018;57:7089–93.
[27] Wei B, Jian S. Analog of midinfrared electromagnetically induced-transparency and slow rainbow trapping light based on graphene nanoribbon-coated silica substrate. J Nanophoton 2017;11(2):026011. https://doi.org/10.1117/1.JNP.11.026011.
[28] Xu Z, Shi J, Davis RJ, Yin X, Sievenpiper DF. Rainbow trapping with long oscillation lifetimes in gradient magnetoinductive metasurfaces. Phys Rev Appl 2019;12(2). https://doi.org/10.1103/PhysRevApplied.12.024043.
[29] Gan Q, Ding YJ, Bartoli FJ. "Rainbow" trapping and releasing at telecommunication wavelengths. Phys Rev Lett 2009;102(056801).
[30] Luo L, Wang K, Ge C, Guo K, Shen F, Yin Z, et al. Actively controllable terahertz switches with graphene-based nongroove gratings. Photon Res 2017;5(6):604. https://doi.org/10.1364/PRJ.5.000604.
[31] Kurt H, Yilmaz D. Rainbow trapping using chirped all-dielectric periodic structures. Appl Phys B 2013;110:411–7.
[32] Neşeli B, Bor E, Kurt H, Turduev M. Rainbow trapping in a tapered photonic crystal waveguide and its application in wavelength demultiplexing effect. J Opt Soc Am B 2020;37(5):1249. https://doi.org/10.1364/JOSAB.388374.
[33] Li C, Wan Y, Zong W. High sensitivity electro-optic modulation of slow light in ellipse rods PC-CROW. Opt Commun 2017;395:188–94.
[34] Chen J, Liang W, Li Z-Y. Switchable slow light rainbow trapping and releasing in strongly coupling topological photonic systems. Photon Res 2019;7(9):1075. https://doi.org/10.1364/PRJ.7.001075.
[35] Fang L, Huiping T, Yuefeng J. A study of dynamic modulation and buffer capability in low dispersion photonic crystal waveguides. J Lightwave Technol 2010;28:1139–43.